Polymer Testing 117 (2023) 107842

Contents lists available at ScienceDirect

Polymer Testing

journal homepage: www.elsevier.com/locate/polytest

Evaluation of methods to accurately characterize the thermal conductivity of micro-and nanocellular polymers based on poly(methyl-methacrylate) (PMMA) produced at lab-scale

Ismael Sánchez-Calderón [a,*], Ángel Sillero [a], Félix Lizalde-Arroyo [a], Victoria Bernardo [b], Judith Martín-de-León [a], Miguel Ángel Rodríguez-Pérez [a,c]

[a] CellMat Laboratory. Campus Miguel Delibes. Faculty of Science. Condensed Matter Physics Department. University of Valladolid, Paseo de Belén 7, 47011, Valladolid, Spain
[b] CellMat Technologies S.L., Paseo de Belén 9-A, 47011, Valladolid, Spain
[c] BioEcoUVA Research Institute on Bioeconomy, University of Valladolid, 47011, Valladolid, Spain

ARTICLE INFO

Keywords:
Nanocellular polymers
Thermal conductivity
Steady-state
Transient

ABSTRACT

The characterization of the thermal conductivity of new and enhanced thermal insulators developed at lab-scale is a challenge. The small dimensions of the prototypes make impossible the use of the conventional techniques because steady-state methods require large samples. Furthermore, the accuracy of transient methods to measure the thermal conductivity is not clear. In this work, we compare four different approaches to measure the thermal conductivity of small prototypes of nanocellular poly(methyl-methacrylate) (PMMA). Both steady-state and transient techniques are used. Results show that the transient plane source method is not suitable for the characterization of these materials (the deviation from the steady-state methods is on average higher than 15%). In addition, two different approaches for measuring the thermal conductivity of small samples via a steady-state technique are proposed and validated.

1. Introduction

Since the development of new and enhanced thermal insulators, like nanocellular polymers or aerogels, is limited to the lab scale and then only small samples are available, the proper characterization of the thermal conductivity of these materials is quite a challenge. This is because commercial equipments based on steady-state techniques, such as guarded hot plates or heat flow meters, require large samples to provide accurate results. The reason is that they are designed to fulfill the requirements of the international standards (such as ASTM C177 [1], ASTM C518 [2], ISO 8301 [3], or ISO 8302 [4]), in which samples with dimensions higher than 100 × 100 mm^2 are required. Meanwhile, transient methods, like transient plane source (TPS), allow measuring samples with smaller dimensions, but its accuracy for thermal insulating materials is not clear [5–7]. For instance, Zheng et al. [6] proved that complex calculations are required to fit the TPS data to more realistic values as those obtained in steady-state techniques. Thus, researchers have been building in-house equipment [8–13] or directly tuning their commercial devices [14] to measure high insulating samples with small sizes. However, there is no standard method to measure those materials easily and comparably for the scientific community. Thus, we have recently developed and validated and steady-state-based method in which we use external heat flux sensors that are incorporated into a commercial heat flow meter for measuring small insulating samples [15].

Regarding the nanocellular materials, it was claimed several times that they could be potentially used as advanced thermal insulators when combining low-densities and nanometric cell sizes [16–18]. For instance, Wang et al. [19] reported 24.8 mW/(m·K) of thermal conductivity (obtained through the TPS method) for nanocellular poly (methyl-methacrylate)/thermoplastic polyurethane (PMMA/TPU) blend characterized by a relative density of 0.125 and 205 nm of cell size. Note that this value is below the air thermal conductivity, which is around 25 mW/(m·K) at 20 °C [20]. The same group also measured with TPS a thermal conductivity of 26.5 mW/(m·K) for nanocellular polyether block amide/polyamide (PEBA/PA) (0.172 of relative density and 176 nm of cell size) [21]. However, regarding nanocellular PMMA, thereafter, it has been demonstrated that such a low thermal

* Corresponding author.
E-mail address: ismaelsc@fmc.uva.es (I. Sánchez-Calderón).

https://doi.org/10.1016/j.polymertesting.2022.107842
Received 8 August 2022; Received in revised form 25 September 2022; Accepted 15 October 2022
Available online 17 October 2022

conductivity cannot be reached [22]. These predictions have been confirmed by recent theoretical [23] and experimental [24] works. Considering these contradictory results, it is clear that the accuracy of the thermal conductivity values measured by using the transient methods for nanocellular polymers is not clear. Therefore, it is mandatory to develop a method to properly characterize these materials and find out their true potential and limitations to be used as thermal insulators.

In this study, the thermal conductivity characterization of nanocellular PMMA, obtained through different methods (steady-state and transient), is reported. Two steady-state approaches able to measure small dimensions samples are analyzed. The first one is based on the use of a mask with a lower thermal conductivity than the sample (the lowest the mask thermal conductivity, the better), while the second one is based on the use of external heat flux sensors as in Ref. [15]. These methods are compared with the conventional steady-state method for large samples and the transient plane source method. Results support that for nanocellular polymers steady-state methods provide accurate results, while TPS overestimates, on average, the conductivity by more than 15%.

2. Experimental

2.1. Materials

The microcellular and nanocellular materials based on PMMA were produced by gas dissolution foaming. Once polished, the resultant samples had dimensions of 50 × 50 × 7 mm^3. Details of the procedure and set-up to fabricate these samples can be found in our previous work [24]. Table 1 summarizes the relative density (ρ_r), cell size (φ_{3D}), and normalized standard deviation of the cell size distribution (SD/φ_{3D}) of the materials used in this work (the characterization methods to obtain these parameters can be found elsewhere [24]). Samples with relative densities in the range of 0.088 and 0.183 have been tested. Cells sizes ranged between 390 nm and 3.7 μm. The cell size distribution of the samples is homogeneous with values of SD/φ_{3D} below 0.70.

2.2. Thermal conductivity characterization techniques

2.2.1. Method HFM: steady-state measurements of large samples using a heat flow meter (reference method)

Steady-state thermal conductivity measurements were carried out using a thermal heat flow meter model FOX 200 (TA Instruments/LaserComp, Inc.), which measures according to ASTM C518 and ISO 8301 [2,3]. Note that the heat flow meter technique is a comparative method to obtain the thermal conductivity since provides results according to a calibration using a material of known thermal conductivity [25,26]. This equipment has been calibrated using a 1450D Standard Reference Material (SRM) (characterized by 33.4 mW/(m·K) of thermal conductivity at 20 °C) issued and certified by the National Institute of Standards and Technology (NIST).

For the measurements, the sample was placed between the two plates, promoting a temperature gradient through the material thickness. The measurement was performed at 20 °C. The temperature gradient was set to 20 °C (i.e., the temperature goes from 10 °C in the upper isothermal plate to 30 °C in the lower one). The active area of the FOX 200 heat flux transducers is 75 × 75 mm^2. The absolute thermal conductivity accuracy for this device is 2%.

Table 1
Relative density, cell size, and normalized standard deviation of the cell size distribution (SD/φ_{3D}) of the nanocellular samples used in this work.

Sample	ρ_r	φ_{3D} (nm)	SD/φ_{3D}
#1	0.088 ± 0.010	1459	0.41
#2	0.095 ± 0.010	3215	0.70
#3	0.097 ± 0.008	1021	0.45
#4	0.098 ± 0.014	2916	0.59
#5	0.129 ± 0.008	468	0.47
#6	0.146 ± 0.008	2379	0.65
#7	0.155 ± 0.007	408	0.47
#8	0.166 ± 0.008	3751	0.67
#9	0.183 ± 0.009	394	0.43

For the reference measurements using the commercial flow meter (HFM), a stack of samples with dimensions of 150 × 150 mm^2 and a thickness of 14 mm [24] was used to conduct the measurements (Fig. 1a). To form the stack, 18 samples of each material as those described in Section 2.1 were used (Fig. 1a). In this case, the stack has larger lateral dimensions than the heat flux transducers, ensuring the accuracy of the measurement. To fill the remaining volume in the heat flow meter cavity, a rigid polyurethane (PUR) foam (characterized by 29.0 mW/(m·K) at 20 °C and 35 kg/m^3) with the same thickness as the stack of PMMA samples was used, avoiding convection. The measurements obtained with this method are considered as the reference value since this is the conventional procedure to characterize insulating materials.

2.2.2. Method M: steady-state measurements of small samples using a heat flow meter and an insulating mask

In this case, two samples were stacked together to result in a sample of 50 × 50 × 14 mm^3 (two samples are used to achieve a higher thickness, for sake of comparison with the reference values). In this method, referred to as mask measurements (M), a PUR mask with 14 mm thickness and a hole of 50 × 50 mm^2 was used and the sample was placed inside the hole. The mask is characterized by a thermal conductivity (λ_{mask}) of 29.0 mW/(m·K) at 20 °C. The mask fills the area (A_{mask}) of the heat flux transducer of the commercial heat flow meter that the sample cannot cover (Fig. 1b). Thus, the resulting total heat flow in the transducers is a sum of the heat flux through the sample and the mask. Therefore, the sample thermal conductivity (λ_{sample_M}) can be obtained according to Equation (1), where λ_{HFM} is the value of the thermal conductivity provided by the commercial heat flow meter, A_{HFM} is the area of the heat flux transducers of the device (75 × 75 mm^2), A_{sample} is the area of the sample (50 × 50 mm^2) and A_{mask} is the area occupied by the PUR mask (the total area of the transducers minus the area of the sample (75 × 75 mm^2–50 × 50 mm^2). The measurement was performed at 20 °C and the temperature gradient of the heat flow meter plates was set to 20 °C.

$$\lambda_{sample_M}(mW/(m\cdot K)) = \frac{\lambda_{HFM}A_{HFM} - \lambda_{mask}A_{mask}}{A_{sample}} = \frac{\lambda_{HFM}75^2 - 29.0\cdot(75^2 - 50^2)}{50^2} \quad (1)$$

Note that in this method, to be able to apply Equation (1), it is very important to use a mask with a thermal conductivity lower but close to the sample to ensure a one-dimension (1D) heat transfer in the two materials and to avoid excessive heat conduction through the mask area.

2.2.3. Method ES: steady-state measurements of small samples using a heat flow meter and two external sensors of small area

The same sample configuration of method M was used here (same sample dimensions and same PU mask), but in this case, the heat flux was measured with two external heat flux sensors, and the temperature on both sides of the samples was measured with two thermocouples (Fig. 1c). The set-up consists of two heat flux sensors gSKIN®-XP 27 9C (greenTEG AG), two data loggers gSKIN® DLOG-4219 (greenTEG AG) to register the sensor data, two silicone rubbers (that minimize the fluctuations of the heat flux measurement), and two type T thermocouples. The set-up is introduced in a heat flow meter, that is used as the heat source. The relative error of the flux measured with the external sensors is 3%. Sensor dimensions are 10 × 10 mm^2 with a thickness of 0.5 mm. The sensor is calibrated under steady-state conditions with a method that is oriented towards ISO8301 [27]. This methodology was described

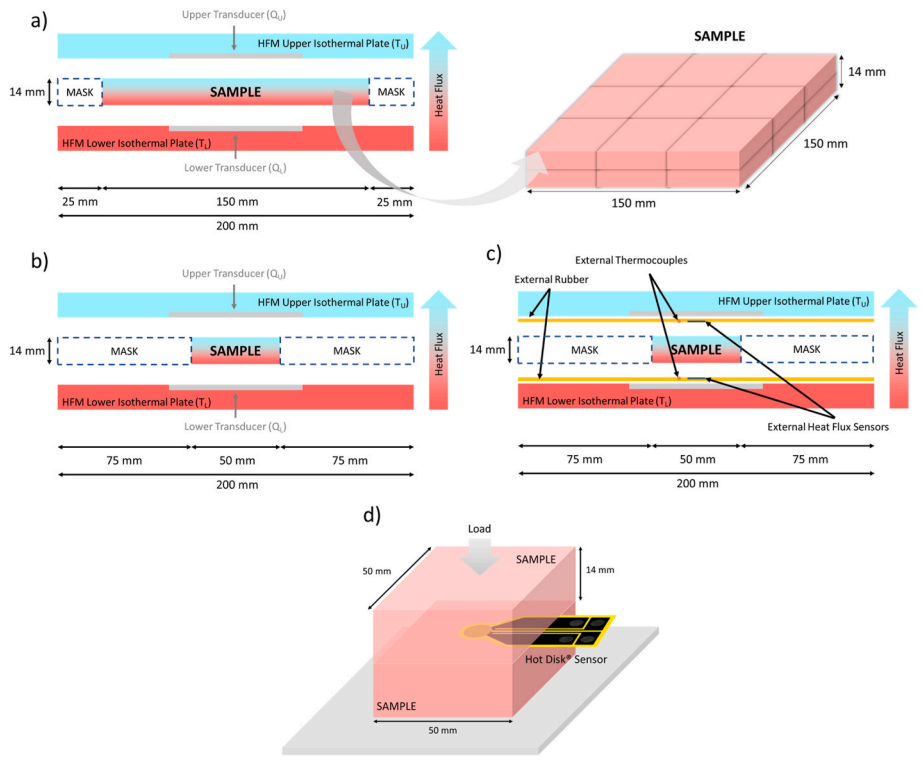

Fig. 1. Scheme of the different methods to measure the thermal conductivity used in this work: a) heat flow meter (HFM), b) mask (M), c) external sensors (ES), and d) transient plane source (TPS).

and validated for different conventional foams in our previous work [15]. In this work, the set-up has been refined. Two sensors are used, and both the sensors and the thermocouples are embedded in the silicone rubbers. With the measurements of the heat flux provided by the heat flux sensors ($\overline{Q}$) and the temperature difference provided by the thermocouples (ΔT), it is possible to calculate the thermal conductivity according to Equation (2), where A_{sample} is the area of the sample and d_{sample} is the sample thickness. The measurement was performed at 20 °C and the temperature gradient of the heat flow meter plates was set to 20 °C.

$$\lambda_{sample_{ES}}(mW/(m\cdot K)) = \frac{\overline{Q}\cdot d_{sample}}{A_{sample}\cdot \Delta T} \tag{2}$$

2.2.4. Method TPS: transient plane source measurements of small samples

A hot-disk transient plane source thermal (TPS) constant analyzer model 2500 S (Hot Disk) was used for the transient isotropic measurements (Fig. 1d). The accuracy of this equipment is 5%. The thermal conductivity measurement was carried out at room temperature (20 ± 2 °C) by stacking four 50 × 50 × 7 mm^3 samples two by two. A disk-shaped TPS Kapton-sensor (code 5501) with a diameter of 6.4 mm was used in all measurements. The sensor was placed between the two stacks of samples. The power output and test duration were 10 mW and 80 s, respectively. The measurement was performed at least 3 times for each sample to calculate, an average value.

2.2.5. Method TPS: correction of the TPS method for low-thermal conductivity materials*

The correction for the TPS measurement developed by Zheng et al. [6] is also used for the sake of comparison and to see if it is applicable to microcellular and nanocellular PMMA. The correction is applied to the results obtained in the method TPS. It is important to remark that this correction is only applicable to sensor 5501 (the one used in this work) since it depends on the sensor characteristics. The equation to calculate the corrected value (λ_{TPS^*}) is given by Equation (3). Where p_{ij} are the coefficients for the polynomial fitting of the correction function (Table 2), $x = ln(\lambda_{TPS})$ and $y = ln(C_{TPS})$. λ_{TPS} is the thermal conductivity in W/(m·K) and C_{TPS} is the volumetric heat capacity in (J/(m^3·K)), both values are obtained in the TPS measurement.

$$\lambda_{TPS^*} = \frac{\lambda_{TPS}}{1 + \sum_{i=0}^{3}\sum_{j=0}^{3} p_{ij}\cdot x^i \cdot y^j} \tag{3}$$

3. Results and discussion

The thermal conductivity results obtained using the commercial heat flow meter (HFM), the mask method (M), the external sensors method (ES), the transient plane source method (TPS), and applying the TPS correction proposed by Zheng et al. [6] (TPS*) are presented in Fig. 2a. Whereas Fig. 2b shows the deviation in % compared to the reference value, method HFM (obtained with the commercial heat flow meter for the sample with higher dimensions than the heat flux transducers). The thermal conductivity of the samples ranges between 38 and 48 mW/(m·K). As deeply studied in our previous work [24], thermal conductivity increases as density increases. However, the nanocellular samples (#3, #7, and #9) do not follow this trend due to their smaller cell size which enhances the Knudsen effect [28], leading to the reduction of the gas thermal conductivity contribution to the total thermal conductivity.

Regarding the methods comparison, it is observed that the M and ES methods provide more accurate results (deviations below 5%) than the

Table 2
Coefficients (p_{ij}) for the polynomial fitting of the correction function.

p_{ij} → i \ j	0	1	2	3
0	−5.524	1.089	−0.07165	0.00158
1	0.6417	−0.09402	0.00358	0
2	−0.01325	0.00394	0	0
3	0.00115	0	0	0

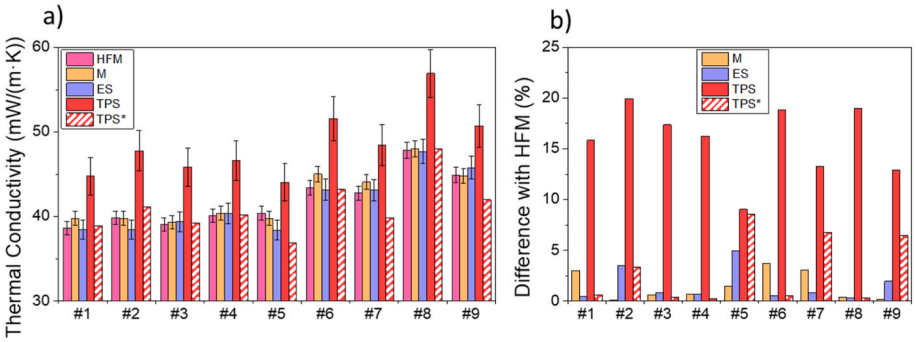

Fig. 2. Results obtained through the commercial heat flow meter (HFM), the mask method (M), the external sensors method (ES), the TPS method, and applying the TPS correction proposed by Zheng et al. [6]. a) Thermal conductivity and b) deviation in % compared to reference measurements (HFM measurements).

TPS. Note that 5% of deviation in this range of thermal conductivity is an absolute deviation of around ±2 mW/(m·K). Furthermore, the error is almost covered by the own accuracy of the methods, which is 2% for the HFM and M methods and 3% for the ES method. Regarding the TPS, it provides higher thermal conductivities in all the cases, with deviations from 9 to 19%, which translate to absolute deviations ranging 3.5–10 mW/(m·K). Meanwhile, when applying the correction proposed by Zheng et al. [6], the results improve approaching the reference values, with maximum differences of 7.3% compared to the HFM reference. It is important to remark that the nanocellular samples (#5, #7, and #9 as shown in Table 1) are the only ones that still present deviations over 5% once the correction is applied.

To summarize, the mask method (M) allows measuring comfortably and precisely the thermal conductivity of small insulating samples using a conventional heat flow meter without any additional investment. However, the main drawback of this method is that the thermal conductivity of the mask must be necessarily lower than the sample to provide accurate results. This fact may complicate using this method for super-insulating samples like aerogels, characterized by thermal conductivities of around 14 mW/(m·K) [29,30]. Regarding the use of the external sensors method (ES), it allows measuring accurately the thermal conductivity of small insulating samples. In this case, the conventional HFM needs to be modified, but the main advantage of this method is that it can be used for any type of material, even for super-insulating materials. Nevertheless, both methods give accurate results with an average difference from the HFM results of 1.5% (which is covered by the relative error of the techniques). Finally, the transient source plate method (TPS) provides thermal conductivity results with a high deviation from the reference value. In our measurements, the values are always high than those measured by the HFM. Therefore, TPS is not a suitable method for characterizing small insulating materials probably due to the large leaks through the thermocouple wires and the current lead wires as reported by Zheng et al. [6]. Those results are improved by applying the correction proposed by Zheng et al. [6], however, for the nanocellular samples, the deviations are still high. These results support that TPS might not be accurate to characterize the thermal conductivity of low-thermal conductivity materials and in particular for microcellular polymers based on PMMA.

4. Conclusions

The thermal conductivity of small samples of microcellular and nanocellular PMMA has been measured through different steady-state and transient techniques. Measurements have revealed that the TPS method is not accurate for the characterization of the thermal conductivity of small samples of nanocellular PMMA, even when the values are corrected considering the sensor characteristics. Meanwhile, for small samples, the external sensor and mask methods are capable to provide comparable results to the ones obtained using large samples and a calibrated commercial heat flow. However, the external sensors method is more appropriate than the mask method since it can be applied to any type of thermal or super-thermal insulator. The discussion here reported may serve for the proper characterization of super thermal insulators with small dimensions.

Author statement

Ismael Sánchez-Calderón: Conceptualization, Investigation, Formal analysis, Writing - Original Draft.

Ángel Sillero: Investigation.

Félix Lizalde-Arroyo: Investigation.

Victoria Bernardo: Conceptualization, Supervision, Writing - Review.

Judith Martín-de-León: Conceptualization, Supervision.

Miguel Ángel Rodríguez- Pérez: Conceptualization, Supervision, Writing - Review, Funding acquisition.

Declaration of competing interest

The authors declare that they have no known competing financial interests or personal relationships that could have appeared to influence the work reported in this paper.

Data availability

Data will be made available on request.

Acknowledgments

Financial support from the Junta of Castile and Leon grant (I. Sánchez-Calderón and VA202P20) is gratefully acknowledged. Financial assistance from the Spanish Ministry of Science, Innovation, and Universities (RTI2018-098749-B-I00 and PTQ2019-010560 (Victoria Bernardo-García)) is gratefully acknowledged. Financial assistance from the European Regional Development Fund of the European Union and the of Castile and Leon ((ICE): R&D PROJECTS IN SMEs: PAVIPEX. 04/18/VA/008 and M-ERA.NET PROJECT: FICACEL. 11/20/VA/0001) is gratefully acknowledged.

References

[1] ASTM C177, Standard Test Method for Steady-State Heat Flux Measurements and Thermal Transmission Properties by Means of the Guarded-Hot-Plate Apparatus, 1997.

[2] ASTM C518 Standard Test Method for Steady-State Thermal Transmission Properties by Means of the Heat Flow Meter Apparatus, 2017.

[3] ISO 8301 Thermal Insulation - Determination of Steady-State Thermal Resistance and Related Properties - Heat Flow Meter, 1991.

[4] ISO 8302 Thermal Insulation - Determination of Steady-State Thermal Resistance and Related Properties - Guarded Hot Plate Apparatus, 1991. https://standards.iteh.ai/catalog/standards/sist/11594d7b-fd5c-45d7-816b- 8e35f1df4d95/iso-4832-1991.

[5] O. Almanza, M.A. Rodríguez-Pérez, J.A. De Saja, Applicability of the transient plane source method to measure the thermal conductivity of low-density

polyethylene foams, J. Polym. Sci., Part B: Polym. Phys. 42 (2004) 1226–1234, https://doi.org/10.1002/polb.20005.
[6] Q. Zheng, S. Kaur, C. Dames, R.S. Prasher, Analysis and improvement of the hot disk transient plane source method for low thermal conductivity materials, Int. J. Heat Mass Tran. 151 (2020), 119331, https://doi.org/10.1016/j.ijheatmasstransfer.2020.119331.
[7] R.C. Kerschbaumer, S. Stieger, M. Gschwandl, T. Hutterer, M. Fasching, B. Lechner, L. Meinhart, J. Hildenbrandt, B. Schrittesser, P.F. Fuchs, G.R. Berger, W. Friesenbichler, Comparison of steady-state and transient thermal conductivity testing methods using different industrial rubber compounds, Polym. Test. 80 (2019), 106121, https://doi.org/10.1016/j.polymertesting.2019.106121.
[8] Y. Jannot, V. Felix, A. Degiovanni, A centered hot plate method for measurement of thermal properties of thin insulating materials, Meas. Sci. Technol. 21 (2010), https://doi.org/10.1088/0957-0233/21/3/035106.
[9] Y. Jannot, A. Degiovanni, V. Grigorova-Moutiers, J. Godefroy, A passive guard for low thermal conductivity measurement of small samples by the hot plate method, Meas. Sci. Technol. 28 (2017), https://doi.org/10.1088/1361-6501/28/1/015008.
[10] Y. Jannot, S. Schaefer, A. Degiovanni, J. Bianchin, V. Fierro, A. Celzard, A new method for measuring the thermal conductivity of small insulating samples, Rev. Sci. Instrum. 90 (2019), https://doi.org/10.1063/1.5065562.
[11] R.A. Miller, M.A. Kuczmarski, Method for measuring thermal conductivity of small highly insulating specimens, J. Test. Eval. 38 (2010), https://doi.org/10.1520/JTE102474.
[12] F. Almeida, H. Beyrichen, N. Dodamani, R. Caps, A. Muller, R. Oberhoffer, Thermal Conductivity Analysis of a New Sub-micron Sized Polystyrene Foam, 2020, https://doi.org/10.1177/0021955X20943101.
[13] C. Zhou, N. Vaccaro, S.S. Sundarram, W. Li, Fabrication and characterization of polyetherimide nanofoams using supercritical CO2, J. Cell. Plast. 48 (2012) 239–255, https://doi.org/10.1177/0021955X12437984.
[14] N. Diascorn, S. Calas, H. Sallée, P. Achard, A. Rigacci, Polyurethane aerogels synthesis for thermal insulation - textural, thermal and mechanical properties, J. Supercrit. Fluids 106 (2015) 76–84, https://doi.org/10.1016/j.supflu.2015.05.012.
[15] I. Sánchez-Calderón, B. Merillas, V. Bernardo, M.Á. Rodríguez-Pérez, Methodology for measuring the thermal conductivity of insulating samples with small dimensions by heat flow meter technique, J. Therm. Anal. Calorim. (2022), https://doi.org/10.1007/s10973-022-11457-7.
[16] S. Costeux, CO2-Blown nanocellular foams, J. Appl. Polym. Sci. 131 (2014), https://doi.org/10.1002/app.41293.
[17] S. Liu, J. Duvigneau, G.J. Vancso, Nanocellular polymer foams as promising high performance thermal insulation materials, Eur. Polym. J. 65 (2015) 33–45, https://doi.org/10.1016/j.eurpolymj.2015.01.039.
[18] C. Forest, P. Chaumont, P. Cassagnau, B. Swoboda, P. Sonntag, Polymer nano-foams for insulating applications prepared from CO2 foaming, Prog. Polym. Sci. 41 (2015) 122–145, https://doi.org/10.1016/j.progpolymsci.2014.07.001.
[19] G. Wang, J. Zhao, L.H. Mark, G. Wang, K. Yu, C. Wang, C.B. Park, G. Zhao, Ultra-tough and super thermal-insulation nanocellular PMMA/TPU, Chem. Eng. J. 325 (2017) 632–646, https://doi.org/10.1016/j.cej.2017.05.116.
[20] Y.A. Cengel, A.J. Ghajar, Heat and Mass Transfer: Fundamentals & Applications, fifth ed., Mc Graw Hill Education, 2006.
[21] J. Zhao, G. Wang, Z. Xu, A. Zhang, G. Dong, G. Zhao, C.B. Park, Ultra-elastic and super-insulating biomass PEBA nanoporous foams achieved by combining in-situ fibrillation with microcellular foaming, J. CO2 Util. 57 (2022), 101891, https://doi.org/10.1016/j.jcou.2022.101891.
[22] G. Wang, C. Wang, J. Zhao, G. Wang, C.B. Park, G. Zhao, Modelling of thermal transport through a nanocellular polymer foam: toward the generation of a new superinsulating material, Nanoscale 9 (2017) 5996–6009, https://doi.org/10.1039/c7nr00327g.
[23] P. Buahom, C. Wang, M. Alshrah, G. Wang, P. Gong, M. Tran, C.B. Park, Wrong expectation of superinsulation behavior from largely-expanded nanocellular foams, Nanoscale (2020), https://doi.org/10.1039/d0nr01927e.
[24] I. Sánchez-Calderón, V. Bernardo, J. Martín-de-León, M.Á. Rodríguez-Pérez, Thermal conductivity of low-density micro-and nanocellular poly(methyl-methacrylate) (PMMA): experimental and modeling, Mater. Des. 221 (2022), 110938, https://doi.org/10.1016/j.matdes.2022.110938.
[25] D. Zhao, X. Qian, X. Gu, S.A. Jajja, R. Yang, Measurement techniques for thermal conductivity and interfacial thermal conductance of bulk and thin film materials, J. Electron. Packag. Trans. ASME. 138 (2016) 1–19, https://doi.org/10.1115/1.4034605.
[26] N. Yüksel, The Review of some commonly used methods and techniques to measure the thermal conductivity of insulation materials, in: Insul. Mater. Context Sustain., 2016, https://doi.org/10.5772/64157.
[27] E.S. Schwyter, T. Helbling, W. Glatz, C. Hierold, Fully automated measurement setup for non-destructive characterization of thermoelectric materials near room temperature, Rev. Sci. Instrum. 83 (2012), https://doi.org/10.1063/1.4737880.
[28] B. Notario, J. Pinto, E. Solorzano, J.A. de Saja, M. Dumon, M.A. Rodríguez-Pérez, Experimental validation of the Knudsen effect in nanocellular polymeric foams, Polymer (Guildf) 56 (2015) 57–67, https://doi.org/10.1016/j.polymer.2014.10.006.
[29] B. Merillas, J.P. Vareda, J. Martín-de León, M.Á. Rodríguez-Pérez, L. Durães, Thermal conductivity of nanoporous materials: where is the limit? Polymers 14 (2022) 2556, https://doi.org/10.3390/polym14132556.
[30] B. Merillas, F. Villafañe, M.Á. Rodríguez-Pérez, Super-insulating transparent polyisocyanurate-polyurethane aerogels: analysis of thermal conductivity and mechanical properties, Nanomaterials 12 (2022) 2409, https://doi.org/10.3390/nano12142409.